The assembly of thiophene-based bis-pyridyl-bis-amide Co^{II} coordination polymers and their polypyrrole-functionalized hybrid materials for boosting their photocatalytic performances

Xiu-Li Wang*, Xiao-Mei Wu, Guo-Cheng Liu, Hong-Yan Lin and Xiang Wang

Department of Chemistry, Bohai University, Liaoning Province Silicon Materials Engineering Technology Research Centre, Jinzhou 121013, P. R. China
Corresponding author: Xiu-li Wang. E-mail address: wangxiuli@bhu.edu.cn (X.-L. Wang)

Table S1 Selected bond distances (Å) and angles (°) for **CP1**–**CP5**.

CP1 $C_{24}H_{20}N_4O_8SCo$			
Co(1)-O(4)	1.999(2)	Co(1)-O(3)	2.026(2)
Co(1)-O(2)	2.132(2)	Co(1)-N(4)	2.169(3)
Co(1)-N(1)	2.188(3)	Co(1)-O(1)	2.277(2)
O(4)-Co(1)-O(3)	120.70(9)	O(4)-Co(1)-O(2)	91.28(9)
O(3)-Co(1)-O(2)	147.97(9)	O(4)-Co(1)-N(4)	90.36(10)
O(3)-Co(1)-N(4)	91.80(9)	O(2)-Co(1)-N(4)	89.73(10)
O(4)-Co(1)-N(1)	86.20(10)	O(3)-Co(1)-N(1)	88.36(9)
O(2)-Co(1)-N(1)	92.21(10)	N(4)-Co(1)-N(1)	176.08(10)
O(4)-Co(1)-O(1)	150.41(9)	O(3)-Co(1)-O(1)	88.89(9)
O(2)-Co(1)-O(1)	59.14(8)	N(4)-Co(1)-O(1)	89.06(10)
N(1)-Co(1)-O(1)	94.85(10)		
CP2 $C_{25}H_{22}N_4O_8SCo$			
Co(1)-O(4)	2.0096(14)	Co(1)-O(3)	2.0172(13)
Co(1)-O(2)	2.1656(13)	Co(1)-N(1)	2.1901(17)
Co(1)-N(4)	2.1943(17)	Co(1)-O(1)	2.2435(15)
O(4)-Co(1)-O(3)	116.71(6)	O(4)-Co(1)-O(2)	96.45(5)
O(3)-Co(1)-O(2)	146.40(5)	O(4)-Co(1)-N(1)	88.95(6)
O(3)-Co(1)-N(1)	95.81(6)	O(2)-Co(1)-N(1)	89.72(6)
O(4)-Co(1)-N(4)	85.65(6)	O(3)-Co(1)-N(4)	89.52(6)
O(2)-Co(1)-N(4)	87.68(6)	N(1)-Co(1)-N(4)	173.70(6)
O(4)-Co(1)-O(1)	155.47(5)	O(3)-Co(1)-O(1)	87.78(5)
O(2)-Co(1)-O(1)	59.37(5)	N(1)-Co(1)-O(1)	87.02(6)

* Corresponding author. Tel.: +86-416-3400158

*E-mail addres*s: wangxiuli@bhu.edu.cn (X.-L. Wang)

N(4)-Co(1)-O(1)	96.56(6)		
CP3 $C_{25}H_{16}N_4O_8SCo$			
Co(1)-O(5)	2.0204(16)	Co(1)-O(6)#1	2.0511(15)
Co(1)-O(2)#2	2.0981(16)	Co(1)-N(1)#3	2.155(2)
Co(1)-N(4)	2.164(2)	Co(1)-O(1)#2	2.3643(16)
O(5)-Co(1)-O(6)#1	125.93(6)	O(5)-Co(1)-O(2)#2	90.08(7)
O(6)#1-Co(1)-O(2)#2	143.99(6)	O(5)-Co(1)-N(1)#3	89.49(8)
O(6)#1-Co(1)-N(1)#3	87.73(7)	O(2)#2-Co(1)-N(1)#3	93.89(7)
O(5)-Co(1)-N(4)	90.16(8)	O(6)#1-Co(1)-N(4)	88.62(7)
O(2)#2-Co(1)-N(4)	90.87(7)	N(1)#3-Co(1)-N(4)	175.22(7)
O(5)-Co(1)-O(1)#2	147.51(6)	O(6)#1-Co(1)-O(1)#2	86.14(6)
O(2)#2-Co(1)-O(1)#2	58.14(6)	N(1)#3-Co(1)-O(1)#2	86.48(7)
N(4)-Co(1)-O(1)#2	96.35(7)		
Symmetry code for **CP3**: #1 2 – x, –y, 1 – z; #2 2 – x, –1 – y, 1 – z; #3 –1 + x, 1 + y, 1 + z			
CP4 $C_{24}H_{19}N_5O_{10}SCo$			
Co(1)-O(6)	2.0258(17)	Co(1)-O(5)	2.0332(16)
Co(1)-N(4)	2.1801(19)	Co(1)-N(1)	2.1814(19)
Co(1)-O(2)	2.1885(18)	Co(1)-O(1)	2.2510(18)
O(6)-Co(1)-O(5)	115.67(6)	O(6)-Co(1)-N(4)	86.85(6)
O(5)-Co(1)-N(4)	89.78(6)	O(6)-Co(1)-N(1)	88.69(6)
O(5)-Co(1)-N(1)	94.92(6)	N(4)-Co(1)-N(1)	174.58(6)
O(6)-Co(1)-O(2)	96.34(6)	O(5)-Co(1)-O(2)	147.72(6)
N(4)-Co(1)-O(2)	87.85(6)	N(1)-Co(1)-O(2)	89.60(6)
O(6)-Co(1)-O(1)	155.67(6)	O(5)-Co(1)-O(1)	88.64(6)
N(4)-Co(1)-O(1)	94.61(6)	N(1)-Co(1)-O(1)	88.20(6)
O(2)-Co(1)-O(1)	59.52(5)		
CP5 $C_{24}H_{20}N_4O_8SCo$			
Co(1)-O(2)#1	2.019(2)	Co(1)-O(1)	2.024(2)
Co(1)-O(3)#2	2.145(2)	Co(1)-N(1)	2.182(3)
Co(1)-N(4)#3	2.183(3)	Co(1)-O(4)#2	2.264(3)
O(2)#1-Co(1)-O(1)	118.41(10)	O(2)#1-Co(1)-O(3)#2	91.66(10)
O(1)-Co(1)-O(3)#2	149.90(10)	O(2)#1-Co(1)-N(1)	88.36(11)
O(1)-Co(1)-N(1)	94.94(11)	O(3)#2-Co(1)-N(1)	86.80(10)
O(2)#1-Co(1)-N(4)#3	83.96(11)	O(1)-Co(1)-N(4)#3	90.69(11)
O(3)#2-Co(1)-N(4)#3	91.18(10)	N(1)-Co(1)-N(4)#3	172.00(11)
O(2)#1-Co(1)-O(4)#2	149.53(9)	O(1)-Co(1)-O(4)#2	90.86(9)
O(3)#2-Co(1)-O(4)#2	59.22(9)	N(1)-Co(1)-O(4)#2	97.93(10)
N(4)#3-Co(1)-O(4)#2	87.64(10)		
Symmetry code for **CP5**: #1 –x, –y, 1 – z; #2 x, y, –1 + z; #3 1 – x, 1/2 + y, 3/2 – z			

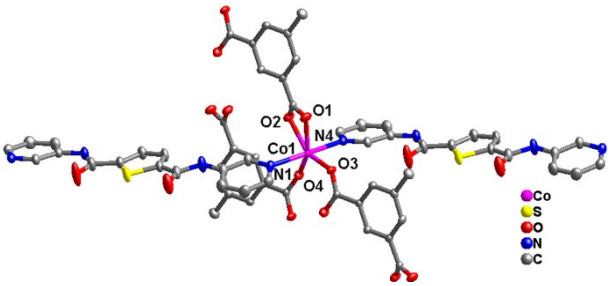

(a)

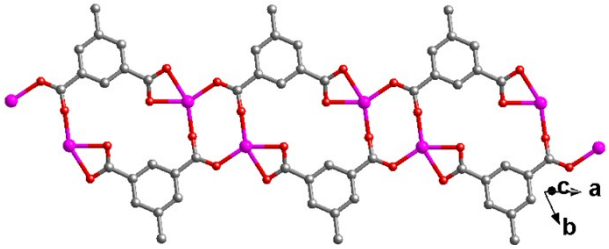

(b)

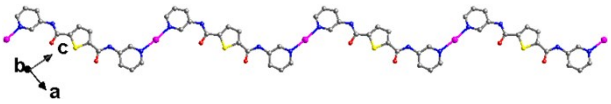

(c)

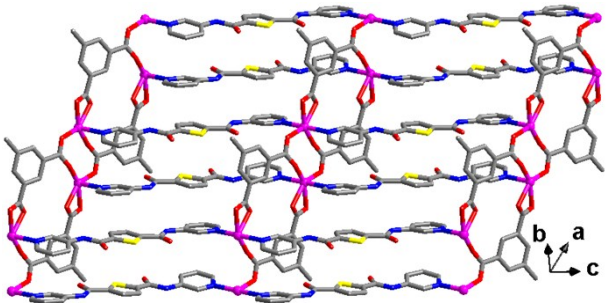

(d)

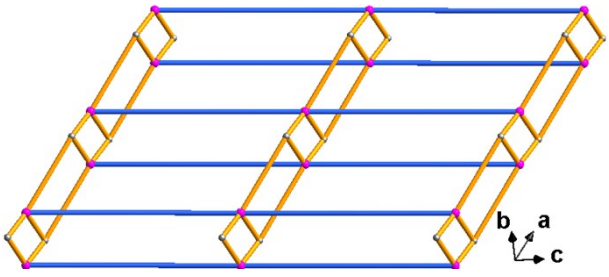

(e)

Fig.S1 (a) Coordination environment of Co^{II} ion in **CP2**. All H atoms and lattice water molecules are omitted for clarity. (b) The 1D ladder-like $[Co_2(5\text{-MIP})_2]_n$ chain in **CP2**. (c) The 1D $[Co(3\text{-bptpa})]_n$ wave-like chain in **CP2**. (d) 2D layer of **CP2**. (e) Simplification of the 3,5-connected network.

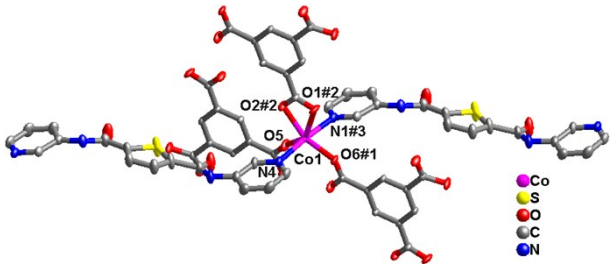

(a)

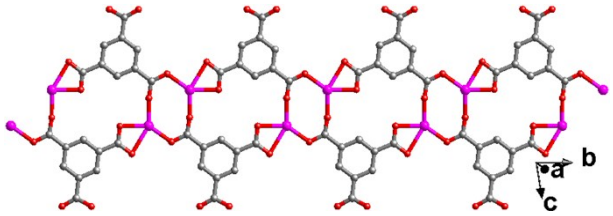

(b)

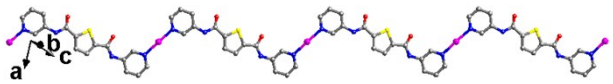

(c)

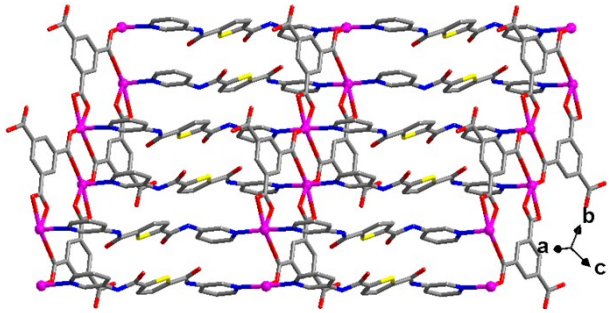

(d)

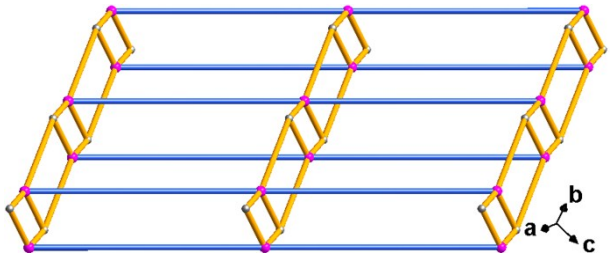

(e)

Fig.S2 (a) Coordination environment of Co^{II} ion in **CP3**. All H atoms and lattice water molecules are omitted for clarity (#1 2 – x, –y, 1 – z; #2 2 – x, –1 – y, 1 – z; #3 –1 + x, 1 + y, 1 + z). (b) The 1D ladder-like $[Co_2(1,3,5\text{-HBTC})_2]_n$ chain in **CP3**. (c) The 1D $[Co(3\text{-bptpa})]_n$ wave-like chain in **CP3**. (d) 2D layer of **CP3**. (e) Simplification of the 3,5-connected network.

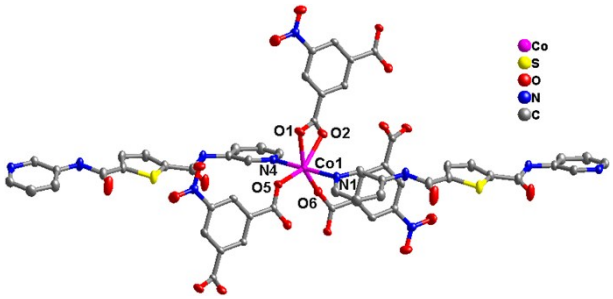

(a)

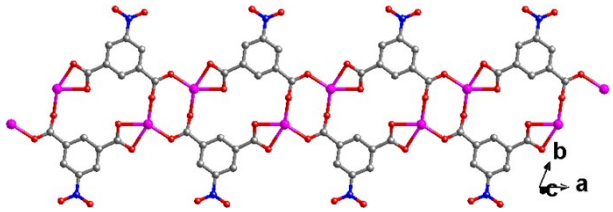

(b)

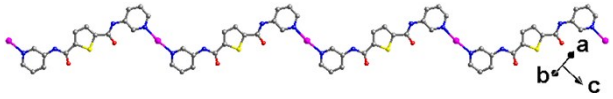

(c)

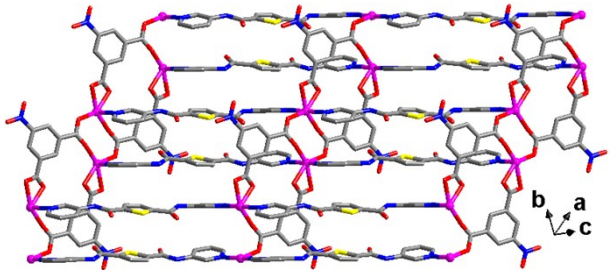

(d)

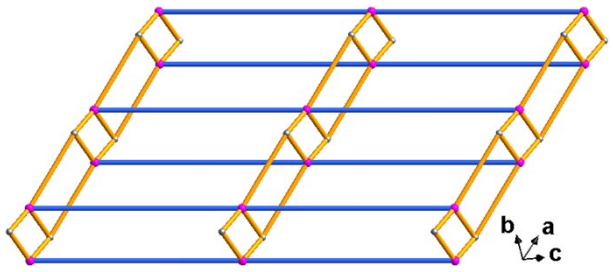

(e)

Fig.S3 (a) Coordination environment of Co^{II} ion in **CP4**. All H atoms and lattice water molecules are omitted for clarity. (b) The 1D ladder-like $[Co_2(5\text{-}NIP)_2]_n$ chain in **CP4**. (c) The 1D $[Co(3\text{-}bptpa)]_n$ wave-like chain in **CP4**. (d) 2D layer of **CP4**. (e) Simplification of the 3,5-connected network.

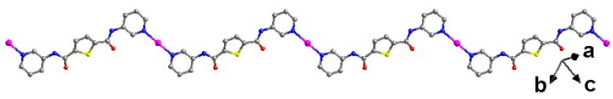

Fig. S4 The 1D $[Co(3\text{-}bptpa)]_n$ wave-like chain in **CP1**.

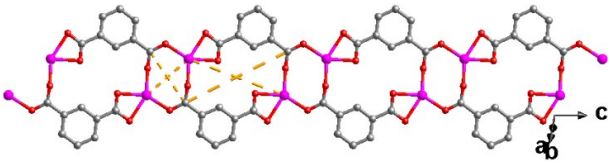

Fig. S5 1D binuclear subunits-containing $[Co_2(1,3\text{-BDC})_2]_n$ chain in **CP5**.

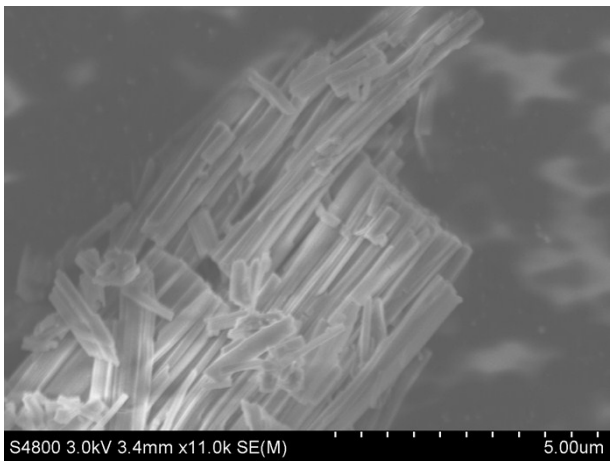

(a)

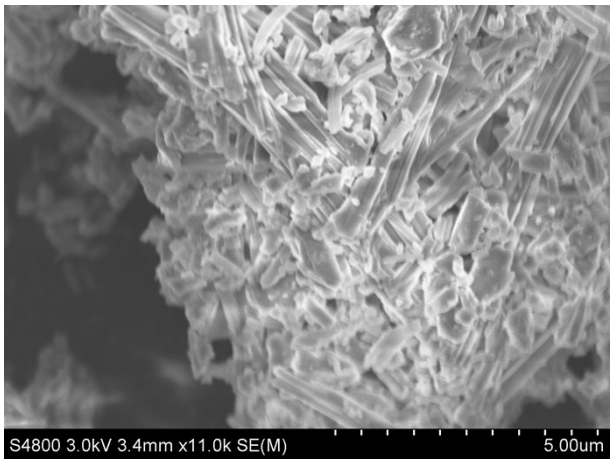

(b)

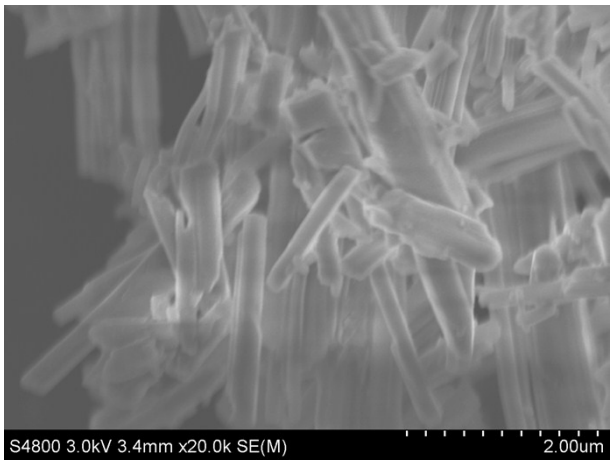

(c)

(d)

(e)

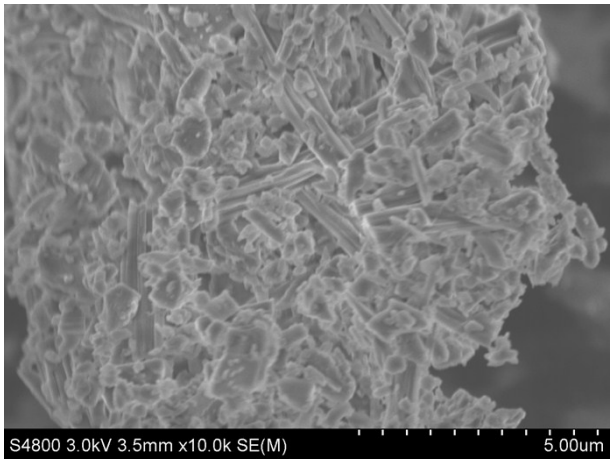

(f)

Fig. S6 SEM pictures of micro-size particles of **CP1** (a), **PPy/CP1** (b), **CP3** (c), **PPy/CP3** (d), **CP5** (e) and **PPy/CP5** (f).

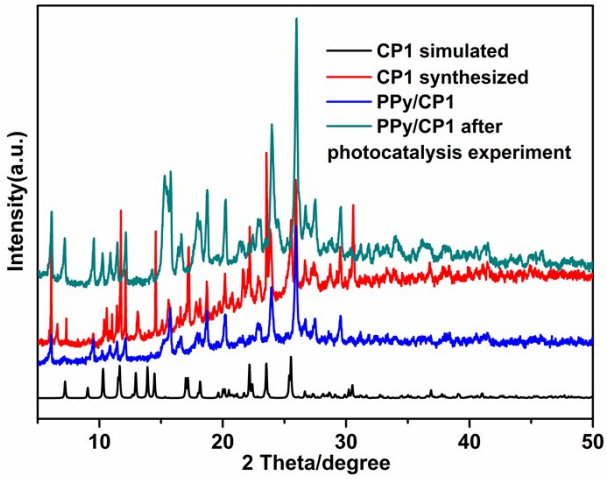
CP1 simulated
CP1 synthesized
PPy/CP1
PPy/CP1 after
photocatalysis experiment
Intensity(a.u.)
10
20
30
40
50
2 Theta/degree

(a)

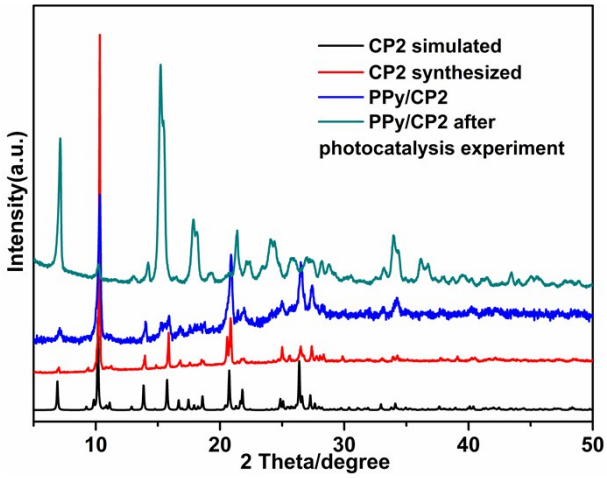
CP2 simulated
CP2 synthesized
PPy/CP2
PPy/CP2 after
photocatalysis experiment
Intensity(a.u.)
10
20
30
40
50
2 Theta/degree

(b)

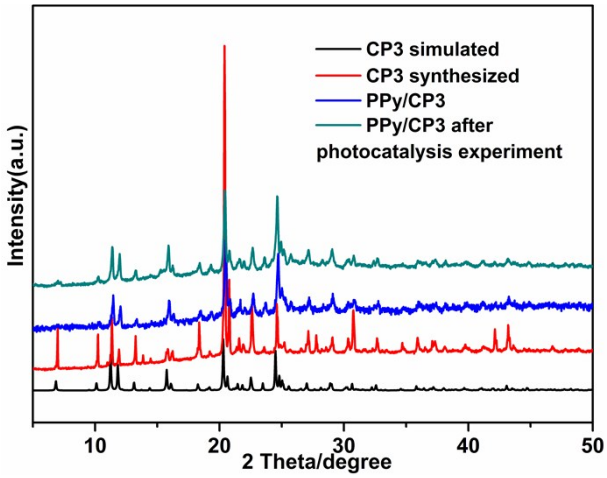
CP3 simulated
CP3 synthesized
PPy/CP3
PPy/CP3 after
photocatalysis experiment
Intensity(a.u.)
10
20
30
40
50
2 Theta/degree

(c)

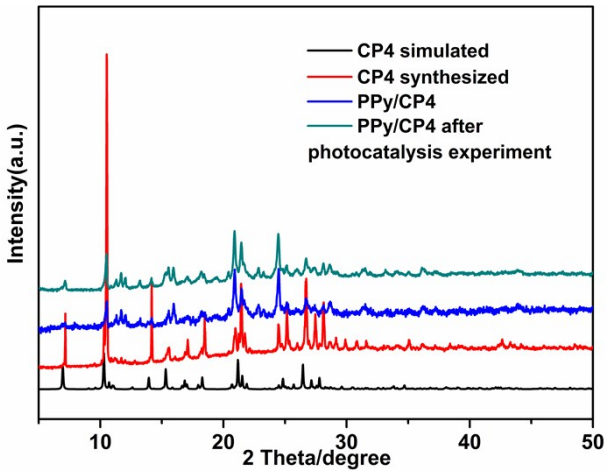

(d)

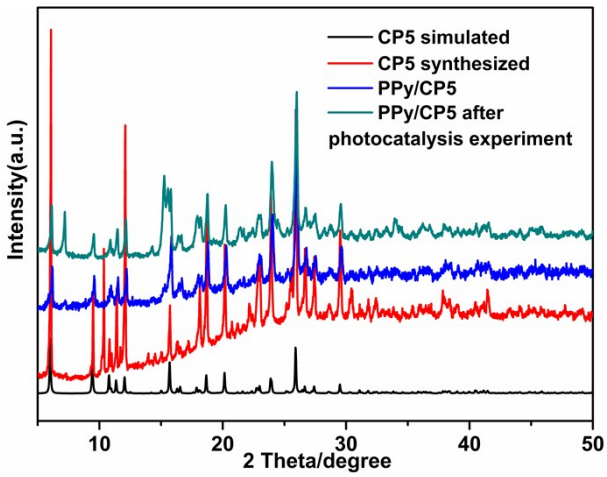

(e)

Fig. S7 The PXRD patterns of **CP1**–**CP5**, **PPy/CP1**–**PPy/CP5** hybrid materials and **PPy/CP1**–**PPy/CP5** after photocatalytic processes.

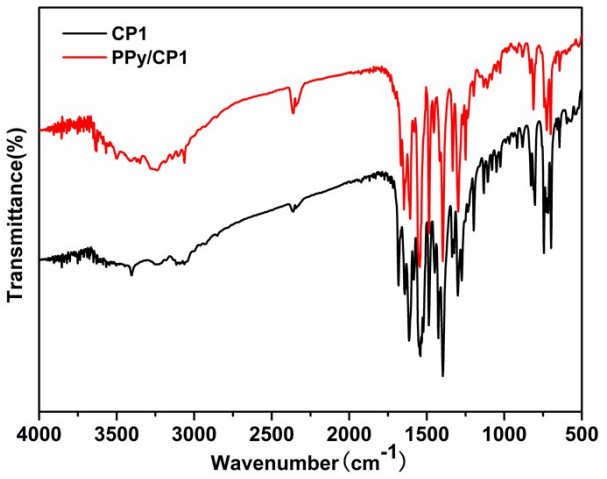

(a)

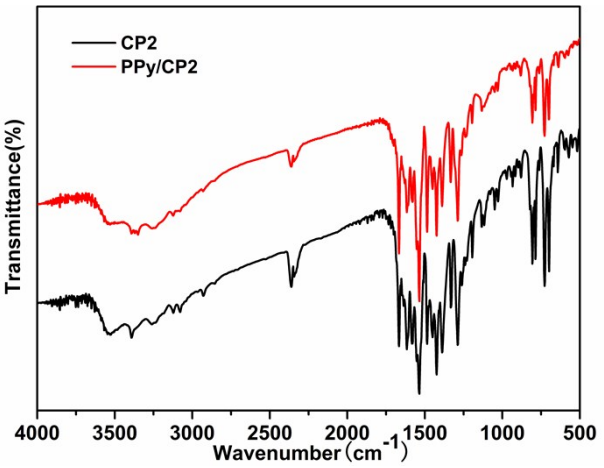
CP2
PPy/CP2
Transmittance(%)
4000 3500 3000 2500 2000 1500 1000 500
Wavenumber (cm-1)

(b)

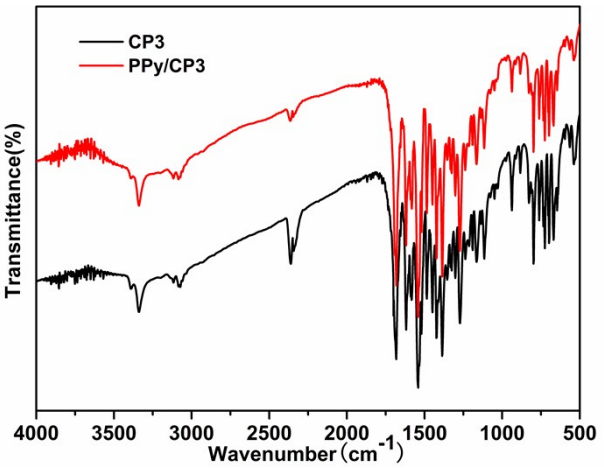
CP3
PPy/CP3
Transmittance(%)
4000 3500 3000 2500 2000 1500 1000 500
Wavenumber (cm-1)

(c)

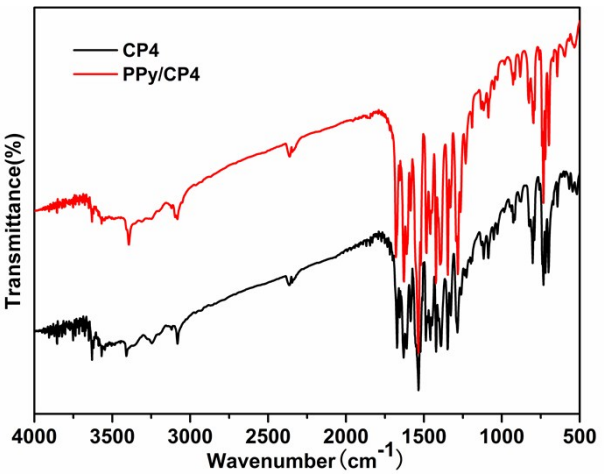
CP4
PPy/CP4
Transmittance(%)
4000 3500 3000 2500 2000 1500 1000 500
Wavenumber (cm-1)

(d)

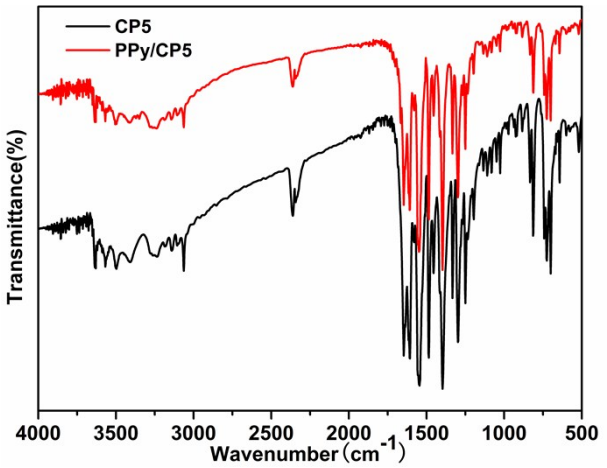

(e)

Fig. S8 The IR spectra of **CP1–CP5** and their **PPy/CP1–PPy/CP5** hybrid materials.

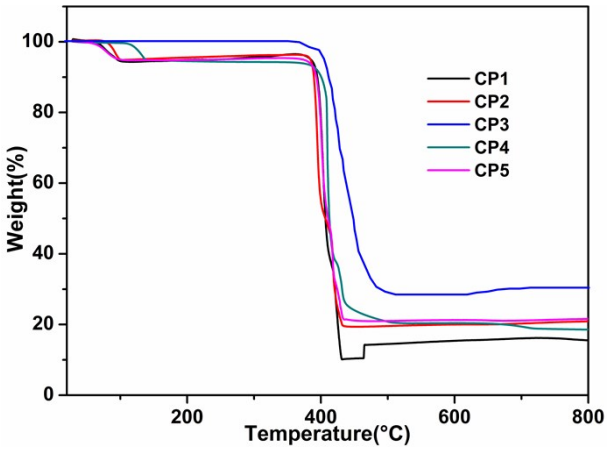

Fig. S9 The TG curves of **CP1–CP5**.

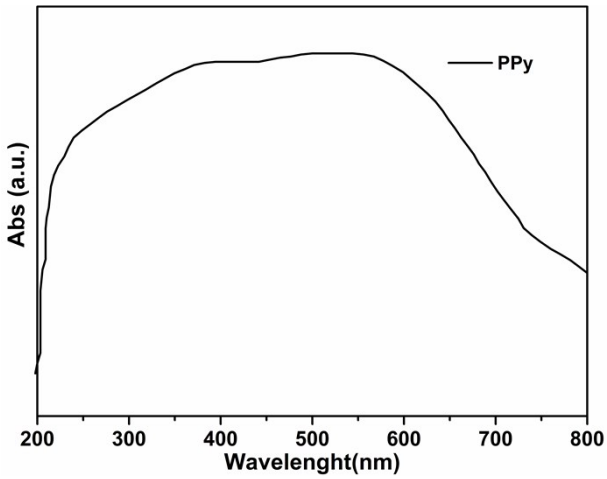

(a)

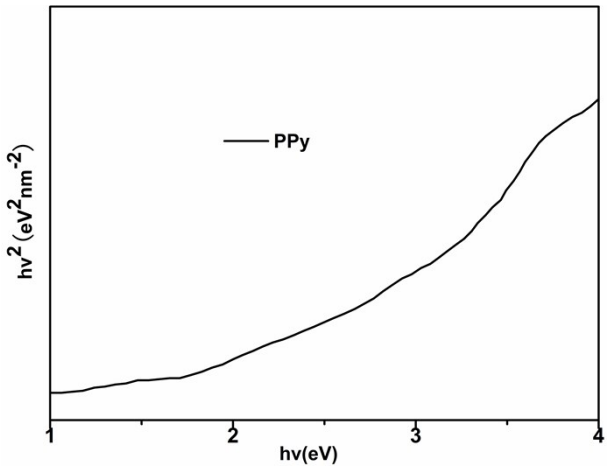

(b)

Fig. S10 The UV−vis diffuse-reflectance spectra (a) and the Tauc plots of the pure **PPy**.

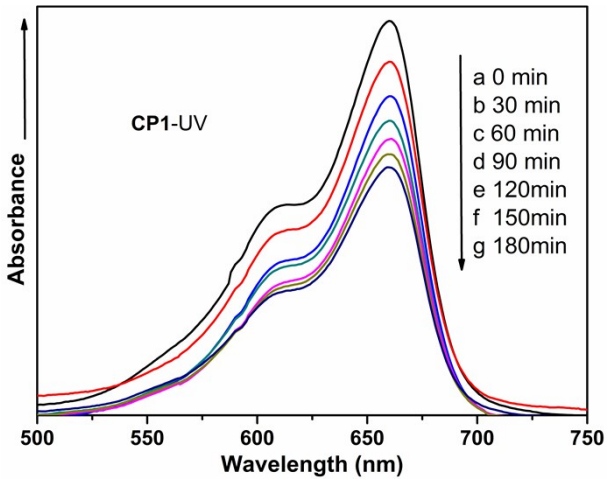

(a)

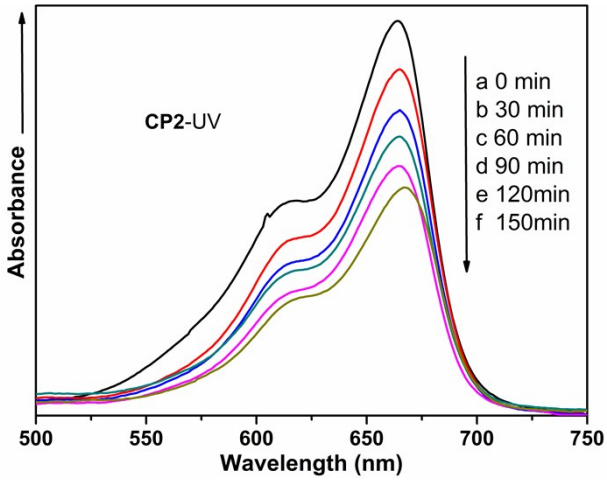

(b)

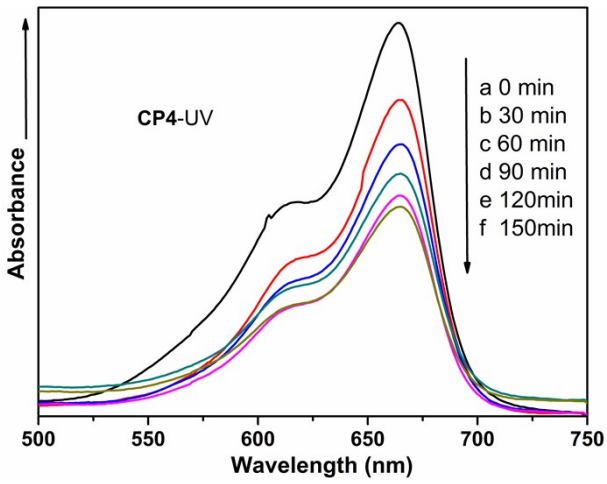

(c)

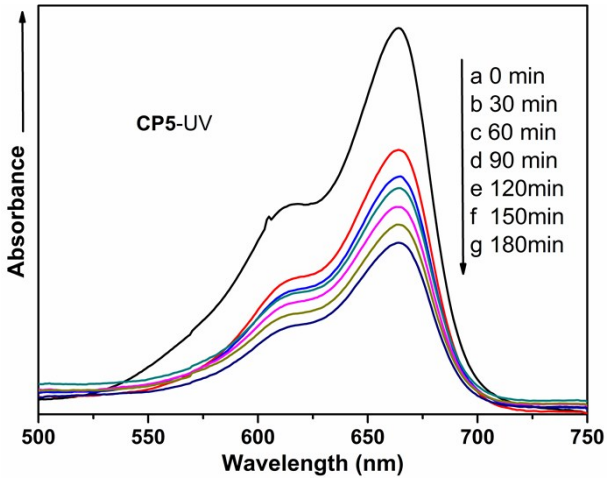

(d)

Fig. S11 Absorption spectra of the MB solution during the decomposition reaction under UV irradiation in the presence of **CP1**–**CP2** and **CP4**–**CP5**.

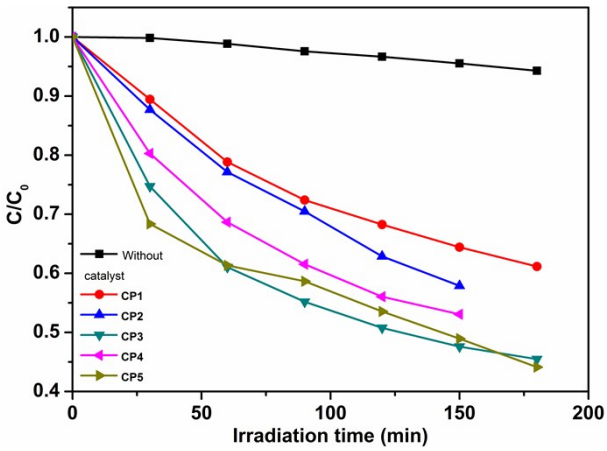

Fig. S12 The degradation ratio of MB for **CP1**–**CP5** under UV light irradiation.

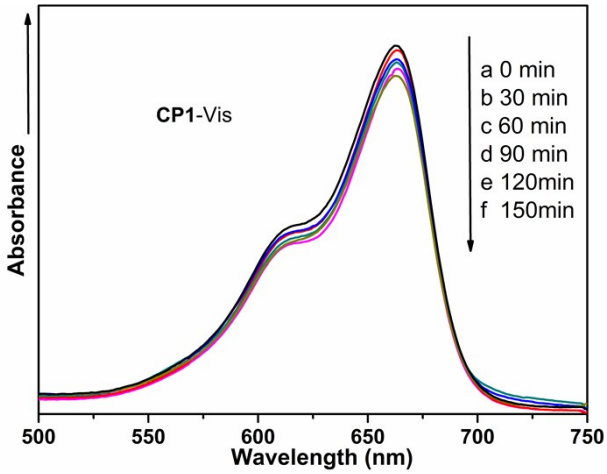
CP1-Vis
a 0 min
b 30 min
c 60 min
d 90 min
e 120min
f 150min
Absorbance
500
550
600
650
700
750
Wavelength (nm)

(a)

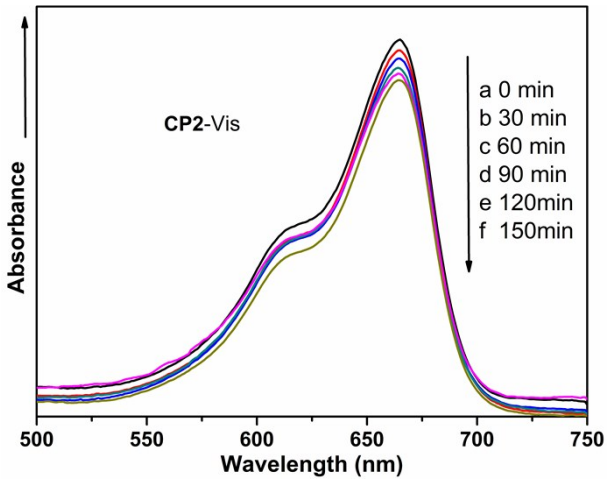
CP2-Vis
a 0 min
b 30 min
c 60 min
d 90 min
e 120min
f 150min
Absorbance
500
550
600
650
700
750
Wavelength (nm)

(b)

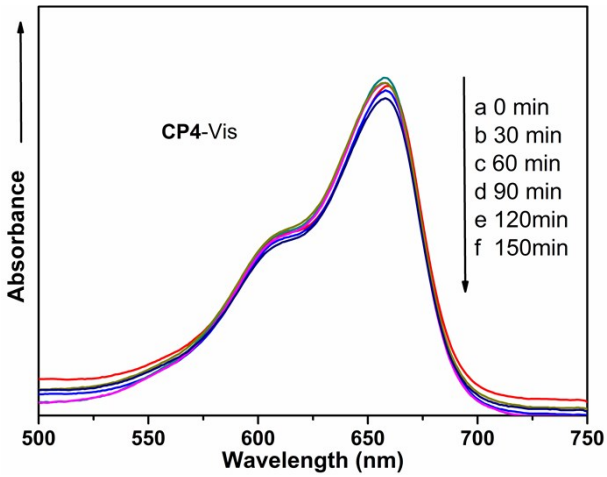
CP4-Vis
a 0 min
b 30 min
c 60 min
d 90 min
e 120min
f 150min
Absorbance
500
550
600
650
700
750
Wavelength (nm)

(c)

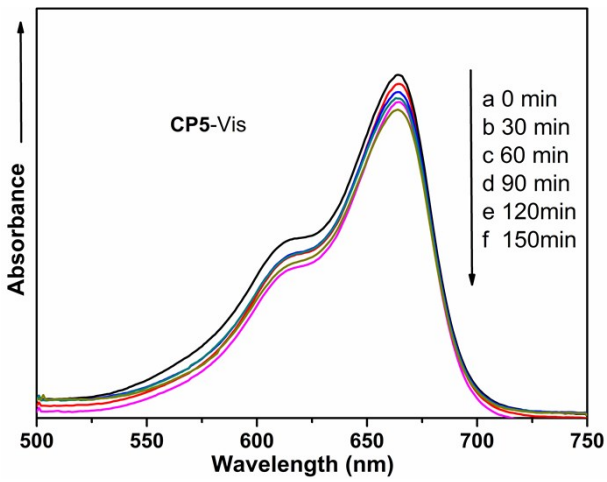

(d)

Fig. S13 Absorption spectra of the MB solution during the decomposition reaction under visible light irradiation in the presence of **CP1–CP2** and **CP4–CP5**.

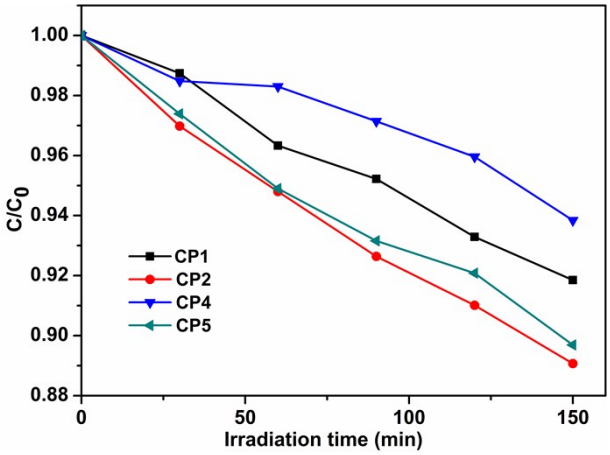

Fig. S14 The degradation ratio of MB for **CP1–CP2** and **CP4–CP5** under visible light irradiation.

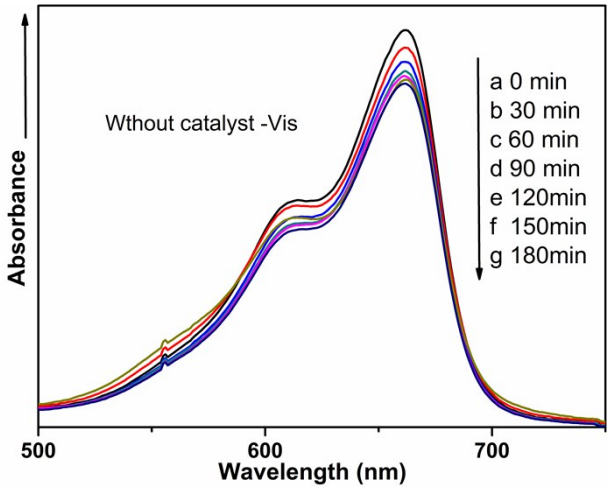

Fig. S15 Absorption spectra of the MB solution during the decomposition reaction under visible light irradiation without photocatalyst.

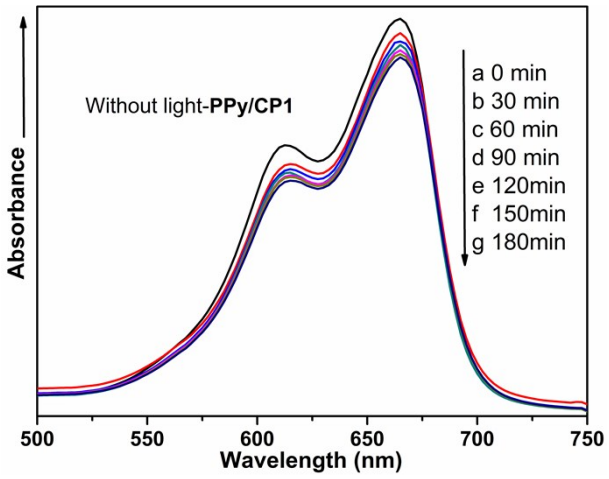
Without light-PPy/CP1
a 0 min
b 30 min
c 60 min
d 90 min
e 120min
f 150min
g 180min
Absorbance
500
550
600
650
700
750
Wavelength (nm)

(a)

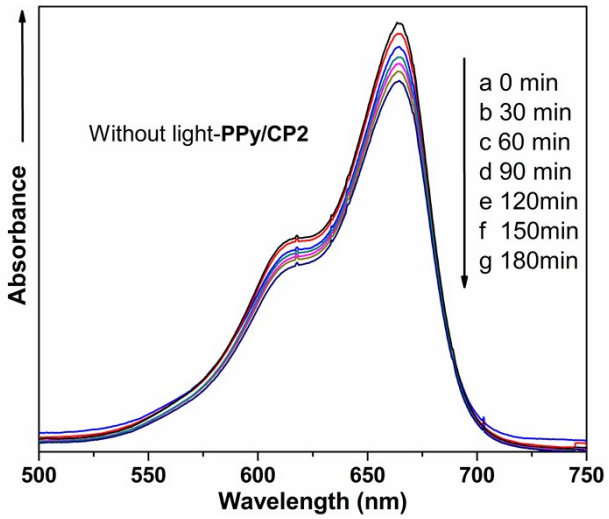
Without light-PPy/CP2
a 0 min
b 30 min
c 60 min
d 90 min
e 120min
f 150min
g 180min
Absorbance
500
550
600
650
700
750
Wavelength (nm)

(b)

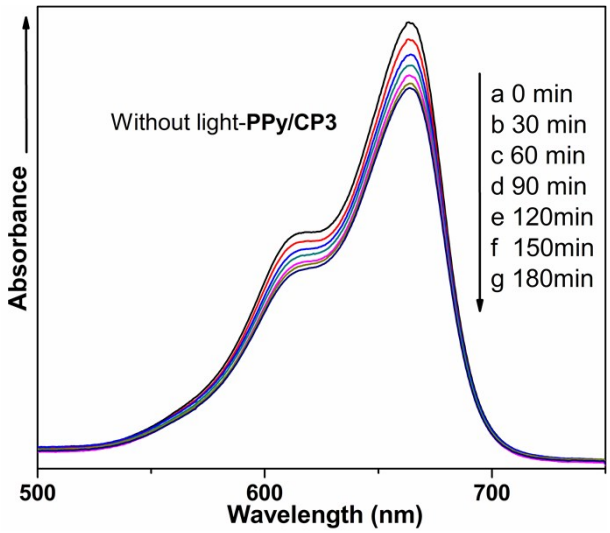
Without light-PPy/CP3
a 0 min
b 30 min
c 60 min
d 90 min
e 120min
f 150min
g 180min
Absorbance
500
600
700
Wavelength (nm)

(c)

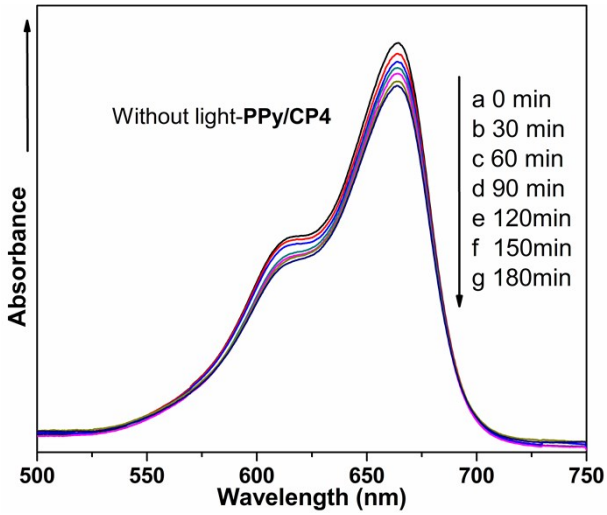

(d)

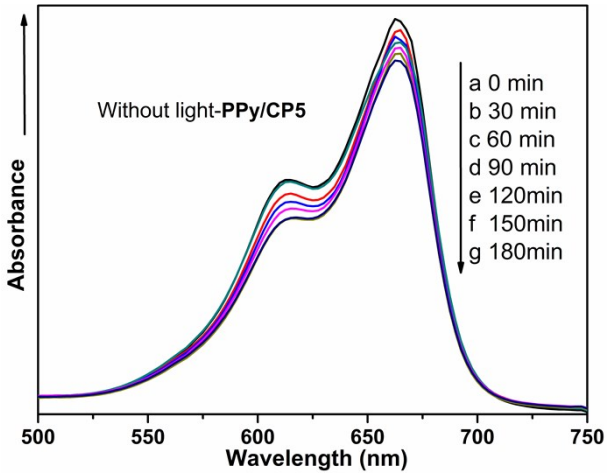

(e)

Fig. S16 Absorption spectra of the MB solution during the reaction without light irradiation in the presence of **PPy/CP1**–**PPy/CP5**.

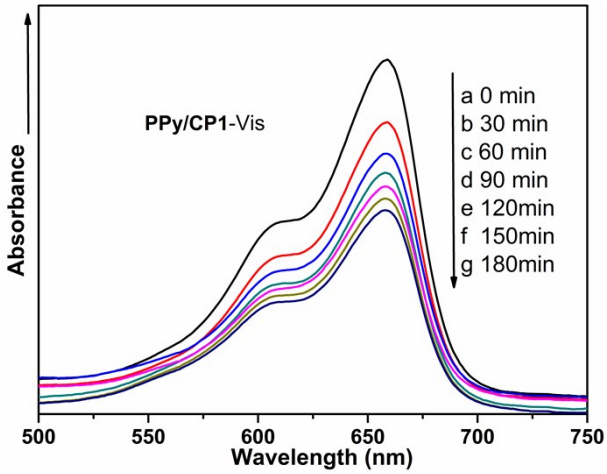

(a)

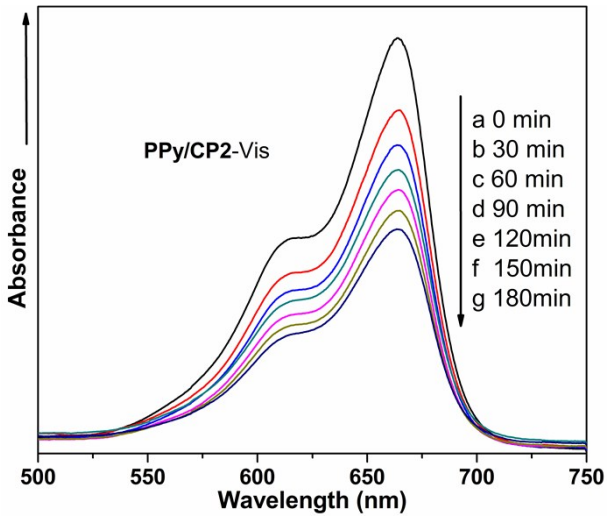
PPy/CP2-Vis
a 0 min
b 30 min
c 60 min
d 90 min
e 120min
f 150min
g 180min
Absorbance
500
550
600
650
700
750
Wavelength (nm)

(b)

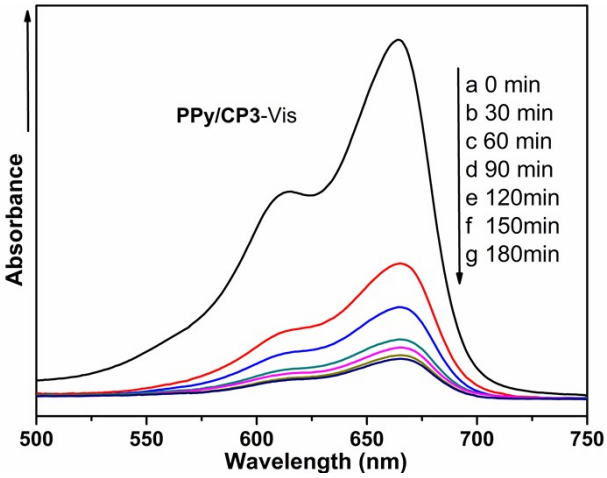
PPy/CP3-Vis
a 0 min
b 30 min
c 60 min
d 90 min
e 120min
f 150min
g 180min
Absorbance
500
550
600
650
700
750
Wavelength (nm)

(c)

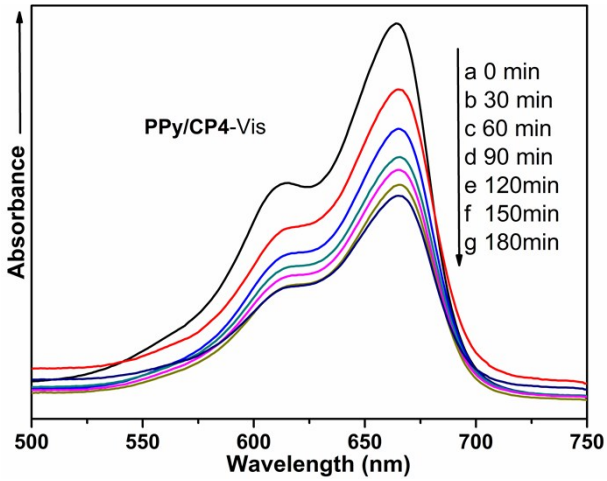
PPy/CP4-Vis
a 0 min
b 30 min
c 60 min
d 90 min
e 120min
f 150min
g 180min
Absorbance
500
550
600
650
700
750
Wavelength (nm)

(d)

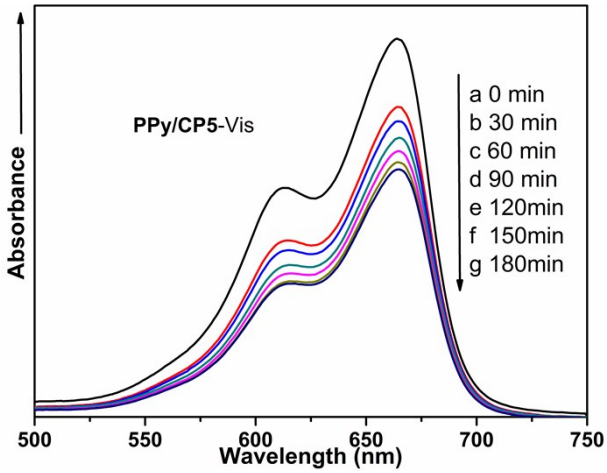

(e)

Fig. S17 Absorption spectra of the MB solution during the decomposition reaction under visible irradiation in the presence of **PPy/CP1–PPy/CP5** hybrid materials.

Fig. S18 The macroscopic photograph during the decomposition reaction under visible irradiation in the presence of **PPy/CP3**.

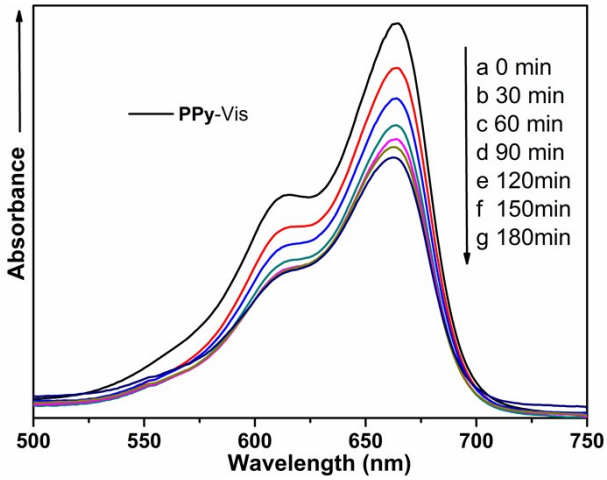

Fig. S19 Absorption spectra of the MB solution during the decomposition reaction under visible irradiation in the presence of pure **PPy**.

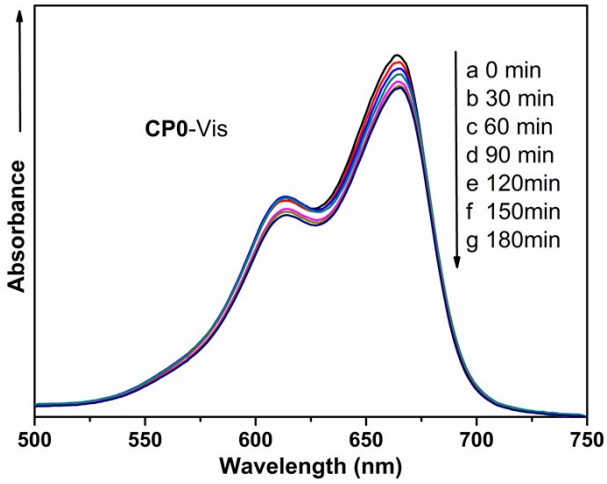

Fig. S20 Absorption spectra of the MB solution during the decomposition reaction under visible irradiation in the presence of a discrete Co(II) complex **CP0**.

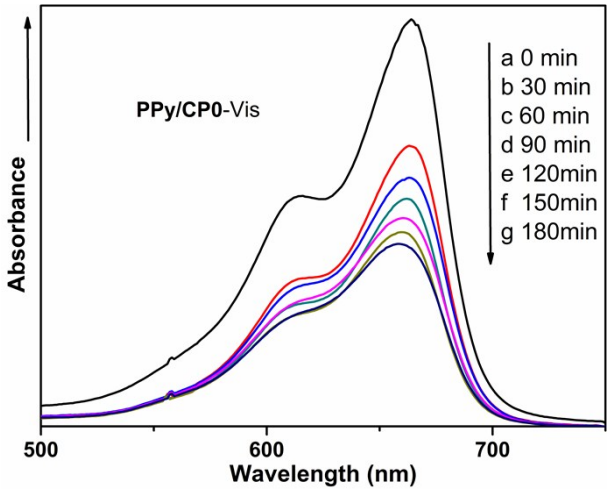

Fig. S21 Absorption spectra of the MB solution during the decomposition reaction under visible irradiation at the presence of a discrete Co(II) complex hybrid material **PPy/CP0**.